ADVANCED ELECTRONIC MATERIALS Open Access
www.advelectronicmat.de



# Reversible Switching of Light-Gated Organic Transistors Employing Dihydroazulene/Vinylheptafulvene Photo-/Thermochromic Molecules

*Sten Gebel, Oumaima Aiboudi, Vladimir Grigorescu, Zhitian Ling, Tomasz Marszalek, Paul W. M. Blom, Charusheela Ramanan, Franziska Lissel, and Ulrike Kraft**

**An innovative possibility to introduce additional functionality to organic field-effect transistors (OFETs) is to employ photochromic molecules, which undergo reversible isomerization under applied stimuli such as irradiation with specific wavelengths. As a result, the transistors not only can be switched on/off by the applied voltages, they can also be programmed by alternate triggers, such as light. Here, reversible switching of OFETs is presented by blending various dihydroazulene/vinylheptafulvene photoswitches into polythiophene-based conjugated polymers. In result, the transfer characteristics of the transistors are altered significantly through UV irradiation. In contrast to current literature on different photoswitches such as spiropyrans or diarylethenes, the backreaction is induced thermally and not via visible light irradiation and reproducibly yields the pristine transistor characteristics. This reversible switching upon alternating UV irradiation and thermal annealing is quantified by figures of merit such as the magnitude of drain current, threshold voltage, and subthreshold swing. Irradiating the devices with different doses of UV light shows that the magnitude of switching directly depends on the respective UV dose, hence enabling a multi-level electronic system. Furthermore, long-term cyclability over 100 steps of repeated UV light exposure and thermal annealing is demonstrated.**

## 1. Introduction

Organic field-effect transistors (OFETs) are a promising platform for next-generation flexible electronics, including bendable displays, stretchable sensor arrays, and on-skin electronics.[1] Impressive improvements in device performance of organic field-effect transistors,[2] as well as operational and environmental stability[3] have opened up the possibility to now focus on the development of more diversified and advanced devices.[4] Multifunctionality is highly desired for organic optoelectronic devices and can be implemented more readily compared to their inorganic counterparts due to the chemical versatility and ease of processing that is inherent to organic electronic materials. Employing photochromic molecules in combination with organic semiconductors is a powerful approach to optically modify electronic device characteristics and add additional functionality, i.e., responsiveness to external stimuli such as light or heat.[5] This concept facilitates a broad spectrum of photo-programmable optoelectronic devices such as photomemory,[6] smart photovoltaic windows[7] or photodiodes for detection of high-intensity ambient light overcoming early photocurrent saturation.[8] Furthermore, it enables multivalued logic, which is highly desirable due to reduced power consumption and increased information density.[4,9]

Photochromic molecules – also called photoswitches – are molecules that undergo reversible isomerization between at least two different (meta)stable isomers upon irradiation with light. This isomerization is oftentimes visible by a change in color

S. Gebel, U. Kraft
Organic Bioelectronics Research Group
Max Planck Institute for Polymer Research
Ackermannweg 10, 55128 Mainz, Germany
E-mail: kraftu@mpip-mainz.mpg.de

The ORCID identification number(s) for the author(s) of this article can be found under https://doi.org/10.1002/aelm.202400455



**DOI: 10.1002/aelm.202400455**

O. Aiboudi, F. Lissel
Leibniz Institute for Polymer Research
Hohe Str. 6, 01069 Dresden, Germany

V. Grigorescu, C. Ramanan
Department of Physics and Astronomy
Vrije Universiteit Amsterdam
De Boelelaan 1081, Amsterdam 1081HV, Netherlands

Z. Ling, T. Marszalek, P. W. M. Blom, C. Ramanan
Molecular Electronics Department
Max Planck Institute for Polymer Research
Ackermannweg 10, 55128 Mainz, Germany

F. Lissel
Technische Universität Hamburg
Kasernenstraße 12, 21073, Hamburg, Germany

and also is accompanied by a change of other fundamental properties such as frontier orbital energy levels, dipole moment, and/or molecular geometry.[10] So far, the most prominent photoswitches in multifunctional organic devices are diarylethenes, spiropyrans/spirooxazines, and azobenzenes.[11] As summarized in several review articles, these molecules have been successfully applied to a range of materials such as small molecule/polymer semiconductors,[12] carbon nanotubes[13] or 2D systems[14] in order to deliberately modify the charge transport in a device. Other photochromic molecules that have been shown to alter charge transport in OFETs upon applying light or thermal stimulus include arylazopyrazole,[15] naphthopyran,[16] and hexaarylbiimidazole[17] compounds.

Several approaches are reported in the literature for incorporating photochromic molecules into OFETs, namely 1) blending them into either the organic semiconductor[18] or the dielectric,[19] 2) interface modification via deposition of a self-assembled monolayer either on the source and drain contacts[20] or at the semiconductor–dielectric interface,[21] 3) via direct covalent incorporation into the semiconductor[22] or the dielectric[23] or 4) as an interlayer between semiconductor and dielectric.[24] Blending the photoswitch into semiconducting polymers is a straightforward approach for creating a photoresponsive active layer material and exploits the good solubility of the polymer and the switch in organic solvents.

A photoswitch that has been studied previously in OFETs is the non-ionic spiropyran (SP), which undergoes isomerization to the zwitterionic merocyanine (MC) under UV light. The latter has been reported to act as a charge scattering site and thus lower the overall current running through a device.[25] It is well known that this isomerization also leads to a considerable change in dipole moment from around 4–6 D for SP to around 14–18 D for MC.[4] This work focuses on a photoswitch with comparable change in dipole moment, but without the presence of any ionic species in either isomer, namely dihydroazulene (DHA)/vinylheptafulvene (VHF) switches, hence enabling to exclusively study the impact of the change in dipole moment on the transistor performance. The isomerization from DHA to VHF can be triggered with UV light and the back reaction from VHF to DHA requires thermal activation enabling a unique mixed photo-/thermochromic system.[26] The actual dipole moments depend on the substitution pattern. However, for a given substituent, the dipole moments of the open VHF form are higher: DHA derivatives typically have dipole moments around 6–10 D, while VHF derivatives show larger dipole moments around 10–15 D.[27] Several reports have been published on how the DHA/VHF isomerization affects the conductance in single-molecule junctions,[28] and on how the dipole moment of single molecules determines the interaction with electric fields,[29] but applications in electronic devices are still scarce.[30] Despite first reports on this particular switch in the nineteen-eighties,[31] the potential of DHA/VHF to tune the electrical characteristics of transistors has not yet been explored. Hence, this work expands the class of stimuli-responsive materials in organic electronic devices beyond the well-established diarylethenes, spiropyrans, and azobenzenes, and takes advantage of the photo/-thermochromic properties of DHA/VHF switches to construct multifunctional electronic devices. Upon applying an organic semiconductor:switch blend as the active layer in an organic field-effect transistor (OFET) the electrical characteristics can be reversibly switched by UV and thermal stimuli. In order to quantify this effect, an in-depth analysis of transistor parameters is carried out and the effect of the UV illumination dose is quantified. DHA/VHF switches with three different substituents are compared and a long-term cyclability of more than 100 illumination/annealing steps is demonstrated.

## 2. Results and Discussion

### 2.1. DHA/VHF Photochromism

The photo-/thermochromism of the DHA/VHF system has been reported for the first time by Daub et al. in 1984.[31a] The reversible isomerization involves a UV light-induced ring-opening reaction from DHA to VHF and a thermally induced ring-closure reaction from VHF back to DHA. The former is typically characterized by a high quantum yield,[32] while the latter is relatively slow with rate constants in the range of $1 \times 10^{-5}$ $s^{-1}$.[32a,33] Both isomers are not only showing different absorption and emission spectra,[32] but also different dipole moment[27] and single-molecule conductance.[28] In this study three different DHA/VHF derivatives were investigated for comparison: 1) with an unsubstituted phenyl ring attached to the C2 position of DHA (DHA/VHF-Ph); 2) with fluorine atoms in both meta-positions of the phenyl ring (DHA/VHF-$F_2$); 3) with a methoxy group in para position (DHA/VHF-OMe). Molecular properties such as ionization potentials, electron affinities, dipole moments and frontier orbitals were determined via DFT calculations and are summarized in Tables S1 and S2 (Supporting Information). **Figure 1a** shows the molecular structure of DHA/VHF-$F_2$ and the characteristic color change between yellow and red upon UV light illumination or heating that can be observed in solution and in thin films. The interconversion between both isomers in solution was studied with UV/Vis absorption- and nuclear magnetic resonance (NMR) spectroscopy. As seen in Figure 1b DHA-$F_2$ absorbs strongly ≈358 nm. With increasing UV irradiation time, the intensity of this absorption band decreases and a new absorption band ≈481 nm starts to appear. This redshift is typical for DHA/VHF compounds and is the signature of the photoinduced conversion from DHA-$F_2$ to VHF-$F_2$. Isosbestic points around 320 and 390 nm indicate that this conversion occurs without any side products. The thermal backreaction in the dark has been monitored using solution NMR spectroscopy. The disappearing multiplet signal of VHF-$F_2$ at a chemical shift of $\delta = 5.14$–5.10 ppm and the appearing signal of DHA-$F_2$ at $\delta = 3.38$ ppm indicates the completed ring-closing reaction from VHF-$F_2$ to DHA-$F_2$.

Pristine films of DHA-$F_2$ show the characteristic yellow color, which turns red upon illumination with UV light (see Figure 1a). A dose as low as 100 mJ $cm^{-2}$ is sufficient to induce this color change, which is the result of DHA transforming into VHF. The photoreaction could be reversed via thermal annealing for 20 min at 90 °C, yielding again the initial yellow-colored film. To further confirm the responsiveness of the photochromic compound in a solid state, transient absorption spectroscopy was carried out on pristine DHA-$F_2$ films, PMMA+DHA-$F_2$ blend films and P3HT+DHA-$F_2$ blend films. In the former two cases the isomerization from DHA to VHF could be observed directly, while in the latter case, no photoexcited interactions between P3HT and

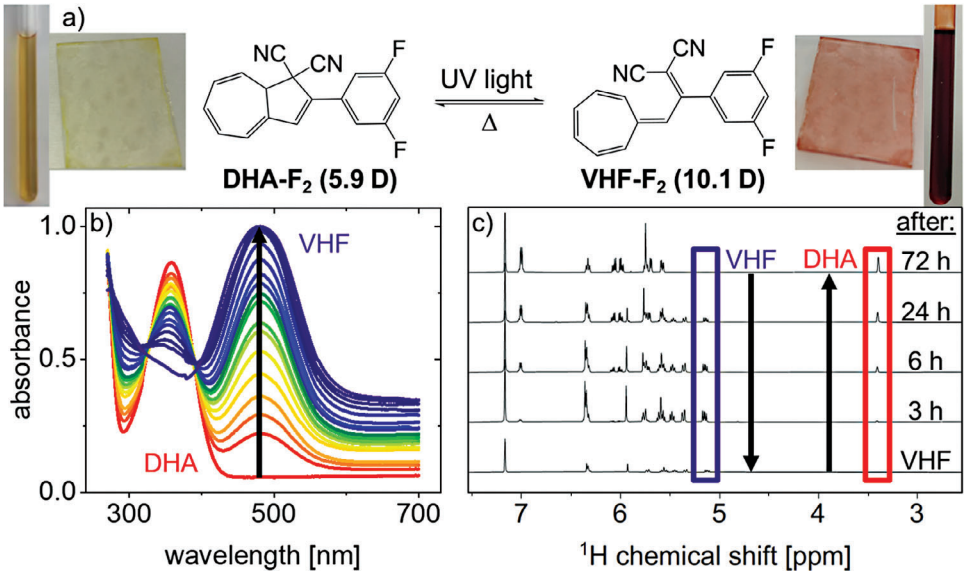


**Figure 1.** The DHA/VHF-$F_2$ photo-/thermochromic system. a) Molecular structures of DHA-$F_2$ and VHF-$F_2$ with the corresponding dipole moments (obtained via DFT calculations). Reversible switching between both isomers is possible via UV illumination (DHA-$F_2$ to VHF-$F_2$) and thermal annealing (VHF-$F_2$ to DHA-$F_2$). The resulting changes in color are demonstrated in solution and thin films of the switch. b) UV–vis absorption spectrum (in solution) indicating the transformation of DHA-$F_2$ (red line) to VHF-$F_2$ (purple line) upon UV illumination. c) NMR spectra (in solution) showing the thermal backreaction of VHF-$F_2$ to DHA-$F_2$ at room temperature over 72 h.

DHA/VHF-$F_2$ could be detected. A detailed discussion of these results is given in the (Section S3 and Figures S2–S4, Supporting Information).

### 2.2. Light-Induced Switching of P3HT+DHA/VHF Blend Transistors

In order to evaluate the switching capability of DHA/VHF in OFETs, the switch was blended into solutions of the semiconducting polymer P3HT, and spin coating was used to fabricate bottom-contact top-gate transistors with Cytop as gate dielectric. Electrical characteristics were recorded after applying UV light illumination and thermal stimuli. A schematic of the organic thin-film transistors and an optical microscopy image are shown in **Figure** 2a. Note that P3HT mainly absorbs in the visible range between 400 and 650 nm,[34] which makes it a suitable host for the DHA-$F_2$ photoswitch that absorbs in the UV range.

It is important to note that measurements were not carried out under illumination, but after switching when the light was turned off. Figure 2b shows the effect of both these stimuli on the transfer characteristics. Figures S8 and S9 (Supporting Information) present a full set of transfer and output characteristics including gate currents (data for a reference device without switch is shown for comparison). These data clearly show that switching can be observed in both transfer and output characteristics. While the transfer characteristics measured after thermal annealing show a clearly defined turn-on voltage around −4 V and a constant level in off-current of around 3 to 4 nA, the curves measured after UV illumination feature a strongly increased off-current, a less defined turn-on voltage, and a noticeably higher on-current. Such behavior might indicate that the VHF form of the switch acts as a dopant, while the DHA form does not (or at least to a lesser degree). A detailed discussion of possible underlying mechanisms can be found below. Figure 2c visualizes how the magnitude of this switching effect depends on the applied UV dose. Different dose levels between 0.1 and 8.3 J $cm^{-2}$ were applied after resetting the switching via annealing (red line). Characteristic transistor parameters such as the on/off-drain currents and subthreshold swing directly depend on the UV dose. We hypothesize that higher UV doses lead to larger magnitude of switching, because a larger population of photoswitches is able to isomerize from DHA to VHF. Similar UV dose dependence effects have been reported in spiropyran and azobenzene-based systems[19a,35] and are probably related to low isomerization quantum yields in solid-state packing.

Such reversible, dose-dependent behavior is highly interesting for multi-level memory devices and can be furthermore exploited in, e.g., UV sensors. For such applications, it is crucial that the same applied stimulus always causes the same response in the electrical characteristics. As shown in Figures S10 and S11 (Supporting Information) different levels in off-current can be repeatedly written and erased in the blend devices. Furthermore, high retention times of the individual memory states and bias stress stability are required. Figure S13 (Supporting Information) shows that the UV-induced increase in off-current is sufficiently stable during 10 h of either negative or positive bias stress. This indicates that the thermal backreaction from DHA to VHF is sufficiently slow in the P3HT blend films under extended electrical bias conditions.

Figure 2d–f shows the reversible switching of transistor parameters over three cycles of UV irradiation and thermal annealing for transistors with and without switch. In the following, such devices will be simply named blend and reference devices respectively. The general trend is that on-current ($|I_D|$ at $V_{GS} = -50$ V) and subthreshold swing increase after UV irradiation, while the

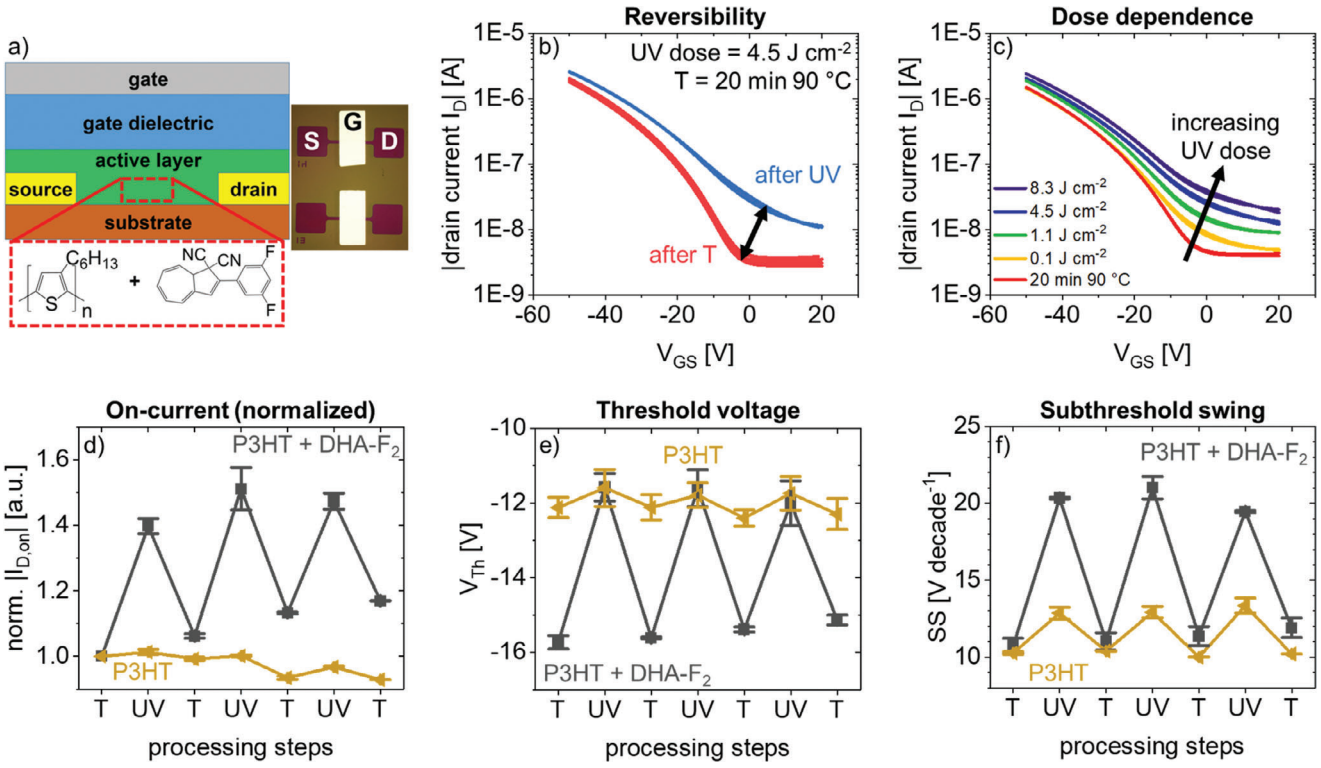


**Figure 2.** Light-gated organic transistors enabled by P3HT blends with DHA/VHF-$F_2$ photo-/thermochromic molecules. a) Schematic illustration of the bottom-contact top-gate OFETs with an active layer containing the organic semiconductor and the switch molecules. b) Reversible switching of transfer characteristics ($V_{DS}$ = −50 V) of blend transistors after repeated UV illumination (4.5 J $cm^{-2}$) and annealing (90 °C for 20 min). c) Dose-dependent switching of multiple electronic states ($V_{DS}$ = −50 V). d–f) Reversible switching of transistor parameters d) normalized on-current, e) threshold voltage, and f) subthreshold swing) extracted from transfer characteristics ($V_{DS}$ = −50 V). Threshold voltage shifts, normalized threshold voltage, normalized subthreshold swing, mobility, and normalized mobility are shown in Figure S5 and S6 (Supporting Information). UV = 4.5 J $cm^{-2}$ and T = 90 °C for 20 min.

threshold voltage shifts to more positive values. It is important to note that also the reference transistors show a response to the applied irradiation, even though all characteristics were measured after the light had been turned off. Such behavior has previously been reported for UV irradiation of P3HT and PBTTT transistors under ambient conditions and was ascribed to the formation of hydrated $O_2(H_2O)_n$ clusters.[36] For our study, the OFETs were kept under glovebox conditions at all times in order to prevent atmospheric doping. However, it is impossible to fully eliminate the adverse effects of $O_2$ and $H_2O$ in organic semiconductor devices with reasonable effort. If not from the atmosphere, residual $O_2$ and $H_2O$ can be, e.g., introduced to the devices via the polymers, switches or processing solvents.[37] Regardless of the exact nature of this effect, our data indicates that this photoinduced doping effect is much smaller than the impact of the photoswitch.

### 2.3. Comparison of P3HT and PBTTT Blend Transistors

After having shown that DHA/VHF-$F_2$ switch molecules facilitate photoresponsive OFETs, a detailed study of the dose dependence of two polythiophene conjugated polymers was carried out. **Figure 3**a,c shows the effect of different doses of UV irradiation on the switching behavior of P3HT blend and PBTTT blend OFETs. Figure 3b,d and Figure S12 (Supporting Information) show the changes in off-current ($|I_D|$ at $V_{GS}$ = 0 V) as a function of UV dose between blend and reference transistors. The increase in off-current as a consequence of illumination with UV light is significantly more pronounced for blend devices than for reference devices These results clearly show that the approach of blending DHA/VHF-$F_2$ into the active channel materials of OFETs is a viable strategy to obtain light-switchable devices and that this approach can be applied to different polymer hosts. Furthermore, the induced switching of OFET characteristics depends directly on the applied UV dose and can be reversed via thermal annealing.

### 2.4. Comparison of Different DHA/VHF Switches

The photophysical behavior of DHA/VHF switches can be altered by attaching different substituents to the five-membered ring in the DHA molecule. Electron-withdrawing groups have been reported to redshift the absorption of VHF, while the opposite trend, i.e., a blueshift has been reported for electron-donating substituents.[32a,38] In order to clarify whether such substituent-effects are also affecting the switchability of OFETs, two other DHA/VHF derivatives were investigated in P3HT blend OFETs. In addition to the previously discussed DHA-$F_2$ switch (see above), where the substituent has electron-withdrawing

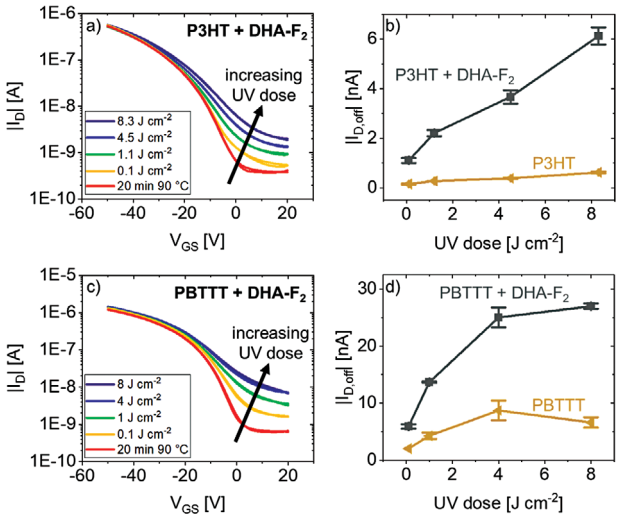


**Figure 3.** The general applicability of the switch to various hosts: Dose-dependent switching of a–b) P3HT blend and c–d) PBTTT blend OFETs. a) and c) Dose-dependent switching of transfer characteristics ($V_{DS} = -5$ V). b) and d) Off-currents extracted from transfer characteristics ($V_{DS} = -5$ V) as a function of UV dose measured on blend and reference devices.

character, one switch with an electron-donating methoxy group (DHA-OMe) and one with an unsubstituted phenyl ring were investigated (DHA-Ph). The molecular structures of these three photo-/thermochromic compounds are shown in **Figure 4a**, while the corresponding ionization potentials, electron affinities, dipole moments, and frontier molecular orbitals are given in Tables S1 and S2 (Supporting Information). All three molecules enable reversible switching of the transistors upon irradiation and annealing. The normalized off-current and subthreshold swing for blend transistors are depicted in Figure 4b,c. A comparison with the reference devices shows that excellent switching can be achieved regardless of the nature of the substituent. However, based on our data it is not possible to establish a clear relationship between the nature of the substituent and the degree of optical switching. Instead, our results show that the fabrication of stimuli-responsive transistors with DHA/VHF switches is a general concept that cannot only be realized with different polymer hosts, but also with various derivatives of the switch. Possibly, further functionalization of DHA/VHF molecules might enable the exploration of a new family of photo-/thermo-responsive optoelectronic devices.

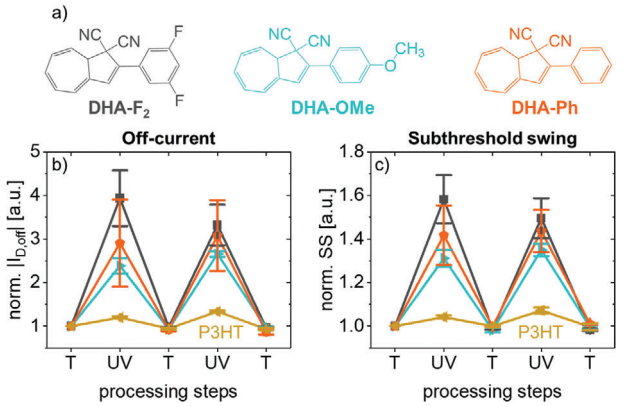


**Figure 4.** Comparison of P3HT blend devices with three different DHA/VHF derivatives. a) Molecular structures of DHA-$F_2$ (black, electron-withdrawing substituents), DHA-OMe (light blue, electron-donating substituent) and DHA-Ph (orange, neither electron-withdrawing or donating substituent). b) and c) Normalized transistor parameters (off-current and subthreshold swing) extracted from transfer characteristics ($V_{DS} = -50$ V). The colors of the lines and symbols match those used for the molecular structures.

## 2.5. Cycling Fatigue and Improved Long-Term Stability

Another important figure of merit for optically switchable OFETs is the long-term cyclability, also called switching fatigue. Diarylethene switches for example are especially resilient to switching fatigue and in some cases coloration and discoloration can be repeated for more than $10^4$ times in solution[39] or in single crystals.[40] Generally, the switching capability of photochromic molecules can deteriorate when they are incorporated into a solid state matrix,[41] which is one possible reason why such high cycle numbers can usually not be reported in blend systems.[42] Due to steric hindrance, it is particularly challenging to achieve sufficient isomerization when the photoswitches are blended into semi-crystalline polymer matrices.[43]

In order to test the long-term cyclability of the novel P3HT blend devices, subsequent irradiation and annealing steps (both steps together comprising one cycle) were carried out and electrical characteristics were recorded every 5 cycles. We believe such long-term studies, especially under applied external stimuli are very valuable in order to properly assess the reliability of such systems. **Figure 5** shows the evolution in off-current and mobility for blend and reference devices over the course of 50 cycles, comprising a total of 103 irradiation/annealing steps. Full sets of transfer and output characteristics (with switch and of the P3HT reference) are given in Figures S14 and S15 (Supporting Information). Moderate switching fatigue of the blend devices manifests itself in 1) a continuous increase in off-current after annealing and 2) an initial decrease in off-current after UV exposure during the first 40 steps, before reaching a plateau. Additionally, the decrease of the charge carrier mobility as a consequence of repeated stimulation was evaluated (see Figure 5b). Average mobilities of around 0.05 and 0.04 $cm^2\ V^{-1}\ s^{-1}$ were determined for the pristine blend and reference devices. As a result of repeated UV exposure and annealing these mobilities decreased

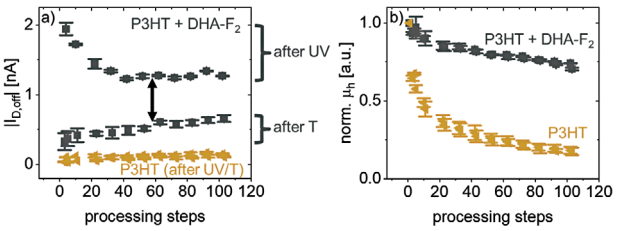


**Figure 5.** Cycling stability: Changes in transistor parameters due to repeated UV illumination and annealing (103 steps in total, but measurements were not carried out after every step) of P3HT blend and reference OFETs. a) Off-currents and b) normalized mobilities extracted from transfer characteristics ($V_{DS} = -5$ V) measured on blend and reference devices.

to 71% and 18% of the initial value for blend and reference devices respectively. Both types of transistors were fabricated, processed, and characterized side by side, the only difference being the presence/absence of the switch. Consequently, not only the increased mobility, but also its enhanced long-term stability can be ascribed to the presence of the switch within the active channel.

To conclude this section, we would like to summarize our key findings: 1) Blending DHA/VHF switches with semiconducting polymers enables light-gated transistors. 2) The degree of switching can be precisely tuned via controlling the applied UV dose. 3) Stimuli-responsive transistors can be fabricated using various polymer hosts and derivatives of the DHA/VHF switch. This indicates the versatility of our approach. 4) Our blend transistors show high resistance against cycling fatigue and significantly reduced degradation of field-effect mobility as a consequence of repeated stimulation when compared to reference transistors.

### 2.6. Discussions

After having shown that DHA/VHF switches enable reversible switching and the programming of multiple states in organic blend transistors, we would like to discuss possible underlying mechanisms. At first it should be noted that we rule out morphology-related effects, since atomic force microscopy (AFM) and grazing-incidence wide-angle X-ray scattering (GIWAXS) data do not show any noticeable change after applied light and thermal stimulus (see Figures S16 and S17, Supporting Information).

As shown above, the blend transistors appear to be doped after UV irradiation (increased bulk conductivity and hole mobility). Furthermore, we observe a decrease in contact resistance as well as sheet resistance after UV light exposure of the blend transistors, which is the typical signature of doping (Figure S19, Supporting Information). However, it is not yet fully clear how the UV-induced VHF derivatives can act as a dopant in a blend with P3HT and PBTTT. Several mechanisms are considered and discussed in the following: 1) Integer charge transfer, 2) (Non-integer) charge transfer via formation of a charge transfer complex, 3) dipole moment-induced photodoping.

In classical integer charge transfer doping, molecules with deep LUMOs can accept electrons from the HOMO of the organic semiconductor, creating additional holes, which contribute to the current in a device. This behavior has been reported for different organic semiconductors in combination with several dopants such as $F_4TCNQ$,[44] $C_{60}F_{48}$[45] or $Mo(tfd)_3$.[46] However, neither DHA-$F_2$, nor VHF-$F_2$ are expected to act as integer charge-transfer dopants, because their electron affinities (2.94 eV for DHA-$F_2$ and 3.17 eV for VHF-$F_2$) are significantly lower than the ionization potentials of P3HT (4.9 eV[47]) and PBTTT (5.1 eV[48]). Another possible mechanism for doping to occur in organic host/guest systems is via the formation of a charge transfer complex (CTC) in which the frontier orbitals of host and guest hybridize to form new occupied bonding and unoccupied antibonding orbitals.[49] These newly formed energy levels can give rise to non-integer charge transfer yielding unpaired electrons. Similar to integer charge transfer doping, these unpaired electrons can be detected with electron paramagnetic resonance (EPR) spectroscopy. In order to investigate whether doping via CTC formation could play a role, EPR spectroscopy was performed on a solution containing P3HT and of VHF-$F_2$. The resulting EPR spectrum is shown in Figure S18 (Supporting Information) and shows no sign of unpaired electrons and hence no evidence for charge transfer between P3HT and VHF-$F_2$ in solution. In addition, the transient absorption spectroscopy results suggest only minimal, if any, photoexcited interactions (i.e., photoinduced charge transfer or energy transfer) between P3HT and the switch. This particular point is discussed in more detail in the Supporting Information (Section S3, Supporting Information).

Interestingly, the close proximity of large dipoles has been reported to induce p-type doping in carbon-nanotubes by Balcı Leinen et al.[50] The authors studied the photoresponsivity of nanohybrids composed of single-walled carbon nanotubes wrapped with conjugated polymers with attached spiropyran moieties and observed an increase in conductivity after UV illumination in two-terminal devices. Under UV light, spiropyran transforms into merocyanine, which is a zwitterionic compound and possesses a larger dipole moment than spiropyran. The observed increase in conductivity of up to two orders of magnitude was ascribed to the large dipole moments of the merocyanine stabilizing positive charges on the nanotubes. This stabilization leads to a localized decrease in ionization potential, which in turn facilitates further doping via atmospheric contaminants such as $O_2$ and $H_2O$. Exciton splitting under illumination might also contribute to this effect. Balcı Leinen et al. suggest that the created holes are stabilized by the large dipoles of the photoswitch and electrons are quenched by atmospheric species. This mechanism is supported by two important findings: 1) The reference devices without any photoswitch also show a (smaller) response to UV light. This response is a lot less pronounced, but still occurs due to the presence of atmospheric contaminants. 2) The response to UV light is cumulative, i.e., longer exposure leads to higher degree of doping, due to the slow backreaction of merocyanine to spiropyran. We also find similar observations in our data. Figure 4, e.g., depicts a noticeable increase in drain current and subthreshold swing of the reference device upon UV irradiation (dark yellow lines). Furthermore, the cumulative effect of UV illumination is well in line with the observed dose dependent modulation of transfer characteristics displayed in Figures 2c and 3.

Despite differences between carbon nanotubes and conjugated polymers, our results show the same fundamental trends as the ones reported by Balcı Leinen et al. and we therefore think it is plausible that similar processes are responsible for the modulations of our transistors. Furthermore, an increase in mobility and drain current caused by additives with significant molecular dipole has been previously observed for polymer transistors as well.[51]

A few other reports on spiropyran/merocyanine photoswitches show increased conductivity or doping effects in a small molecule or conjugated polymer based systems, but lack a consistent explanation.[52] Also, these reports contradict other publications, where the isomerization of spiropyran to merocyanine leads to a deterioration of charge transport.[25] One should however keep in mind that controlled interactions, as reported by Balcı Leinen et al. might lead to different effects compared to a

random distribution of photoswitches within a semiconducting matrix and that the zwitterionic character of merocyanine adds further complexity in contrast to our DHA/VHF system.

Finally, the enhanced ability of the VHF isomer to act as an electron acceptor should be considered. In VHF, the dicyanovinyl group is in conjugation with the $\pi$-electron-system and acts as an electron acceptor due to its strong electronegative character, leading to a stabilization of the VHF isomer and narrowing of the bandgap.[31c] Several studies showed that VHF can be more easily reduced (i.e., accept an additional electron, turning it into its radical anion) than compared to its respective DHA counterpart, making it a light switchable $\pi$-electron acceptor.[53] This functionality has been exploited to modulate photocurrent through an electrochemical cell (higher current with VHF, since it is more readily reduced)[54] or $Na^+$ ion-complexation in covalently attached crown ether moieties (weaker complexation with VHF due to its electron-withdrawing character).[55]

An alternate explanation for the switching of the transistor performance could be trap passivation facilitated by the VHF isomer. Nikolka et al. reported that molecular additives can improve the performance and bias stress stability of organic transistors.[56] The authors suggest that additives containing strong electron-withdrawing moieties, can effectively bind water molecules through hydrogen bonds, thus reducing the number of water-related traps.[57] Interestingly, such trap passivation is mainly observed for additives that feature a dicyanovinyl group in conjugation with a $\pi$-electron-system, as present in the VHF form of our photoswitch.[58]

Taking into account the increase in subthreshold swing upon UV-irradiation, it should also be considered that two effects might be superimposed, and the increase in subthreshold swing results from an increased energetic disorder caused by the increase in molecular dipole moments of the VHF isomers.

## 3. Conclusion

DHA/VHF switch molecules with photo-/thermoresponsive properties were blended into polythiophene-based conjugated polymers to enable novel multifunctional organic transistors, which have high prospects for applications as multi-level memory and synaptic devices. Reversible switching of the current-voltage characteristics due to UV irradiation and thermal annealing was demonstrated and can be attributed to the isomerization between DHA and VHF. To the best of our knowledge, this is the first time that reversible switching of transistors is achieved utilizing DHA/VHF photo-/thermochromic compounds. Transistor parameters such as drain current (in on- and off-state), threshold voltage, and subthreshold swing can be modulated reversibly for three different derivatives of the DHA/VHF switches and the concept is applicable to several polymer matrices. Furthermore, the magnitude of switching depends directly on the applied UV dose enabling multi-level electronic systems. This direct correlation of applied stimulus and modulation of electrical characteristics makes these transistors promising candidates for applications in multi-level photomemories and photodetectors. Furthermore, the presence of the switch also reduces degradation of the field-effect mobility. Finally, a remarkably high resilience to cycling fatigue over 100 steps of repeated UV illumination and thermal annealing was demonstrated.

## 4. Experimental Section

*Materials and Solution Preparation*: DHA/VHF molecular switches were synthesized as described previously.[29a] Regioregular poly(3-hexylthiophene-2,5-diyl) (P3HT, product number 445703, molecular weight = 50–100 kDa) and poly[2,5-bis(3-tetradecylthiophen-2-yl)thieno[3,2-b]thiophene] (PBTTT, product number 753971, molecular weight > 50 kDa) were purchased from Sigma–Aldrich and used without further purification. Stock solutions were prepared with anhydrous chlorobenzene (P3HT, 15 mg $mL^{-1}$) and anhydrous dichlorobenzene (PBTTT, 7 mg $mL^{-1}$) in a nitrogen-filled glovebox and stirred overnight at 60 °C. DHA (molecular switch) was dissolved in the same solvent as the polymer (10 mg $mL^{-1}$) and stirring was performed overnight at room temperature. Solutions for spin coating were prepared by adding either switch stock solution (for blend devices) or pure solvent (for reference devices) to the polymer stock solution. Final polymer concentrations were 10 mg $mL^{-1}$ for P3HT and 5 mg $mL^{-1}$ for PBTTT solutions. The DHA content of the blend solutions was 10 wt.%. Cytop (CTL-809 M) was purchased by AGC Chemicals and used in a volume ratio polymer-solution:solvent of 3:1.[59]

*OFET Fabrication, Characterization and Switching*: Bottom-contact top-gate organic transistors were fabricated on glass substrates. Prior to source/drain electrode deposition, the substrates were cleaned via sonicating in ultrapure water (5 min), acetone, and isopropanol (both 10 min). After drying the substrates in an oven (10 min at 140 °C) a UV/ozone treatment was applied for 20 min. Source and drain electrodes (2 nm chromium as adhesion layer and 30 nm gold, channel length = 30 µm, channel width = 1 mm) were thermally evaporated through shadow masks in vacuum ($<1 \times 10^{-7}$ mbar) After a 20 min UV/ozone treatment the semiconductor:switch blend solutions (or the pure semiconductor solutions) were spin-coated at 1500 rpm for 30 s to yield 35 nm (P3HT) or 20 nm (PBTTT) thin films. Organic semiconductor films were annealed for 30 min at 150 C (P3HT) or 180 C (PBTTT) to remove residual solvent. Afterward, the Cytop gate dielectric was spin coated at 2000 rpm for 20 s on top of the annealed semiconductor film and annealed for 20 min at 90 °C to yield a 500 nm thick dielectric layer. Figure S1 (Supporting Information) shows that the capacitance of the Cytop dielectric is frequency-independent between 1 and $10^5$ Hz and that the dielectric permittivity matches well with the literature value of 2.1. The area-normalized gate dielectric capacitance was calculated to be 3.7 nF $cm^{-2}$. Finally, 70 nm of aluminium were evaporated through shadow masks onto the Cytop as top gate electrodes. All transistors were characterized in the dark (e.g., AFTER light-induced switching) using a Keithley 4200-SCS semiconductor parameter analyzer. Transistor figures of merit, i.e., threshold voltage, subthreshold swing, and field-effect mobility were derived from transfer characteristics following the common procedures described in the literature.[60] The threshold voltage was fitted in the regime $V_{GS} = -30$ to $-50$ V.

The transistors were illuminated using a Dymax ECE 2000 flood lamp (13 mW $cm^{-2}$ at 320–390 nm) and the dose was monitored using a Dymax Accu-Cal 50 UV dose meter. Thermal switching was carried out on a hot plate at 90 °C for 20 min. All fabrication steps from the deposition of the source/drain electrodes onwards, as well as characterization and switching steps were carried out in a nitrogen-filled glovebox.

*Characterization of DHA/VHF in Solution*: Thermal conversion of VHF-$F_2$ to DHA-$F_2$ was monitored via solution $^1$H NMR at room temperature using deuterated benzene as a solvent. The first spectrum was recorded for pure VHF-$F_2$ and all subsequent spectra were recorded after keeping the solution in the dark for 3, 6, 24, and 72 h respectively.

For the UV–vis absorption spectroscopy DHA-$F_2$ was dissolved in acetonitrile. Before the measurement the sample was irradiated outside of the spectrometer, using a UV lamp (500 µW $cm^{-2}$) equipped with a monochromator selecting 365 nm. Spectra were acquired after 2, 7, 10, 13, 17, 22, 30, 40, 60, 70, 85, 100, 125, 150, 175 and 200 s of irradiation. Electron paramagnetic resonance (EPR) spectroscopy was performed on a chlorobenzene solution containing P3HT (10 mg $mL^{-1}$) and 10 wt.% of VHF-$F_2$ (weight fraction calculated from the amount of polymer). Before the measurement, the solution has been irradiated with UV light.

*DFT Studies*: Optimized structures and frontier molecular orbitals of the photo-/thermochromic compounds used in this study were calculated at the B3LYP/6-311G (d,p) level of density functional theory (DFT) using Gaussian09.

*Transient Absorption Spectroscopy*: The pristine films of DHA-$F_2$ and the PMMA+DHA-$F_2$ blend films were fabricated via spin coating from anhydrous chloroform solutions (32 mg $mL^{-1}$ for pristine switch and 40 mg $mL^{-1}$ PMMA+33 wt.% DHA-$F_2$ for PMMA blends). P3HT+DHA-$F_2$ blend films were prepared under the same conditions as the transistor devices.

Femtosecond transient absorption spectra (fs-TAS) were obtained using a Helios Fire pump-probe setup (Ultrafast Systems). This is paired with a regeneratively amplified 1030 nm laser (Pharos, Light Conversion, 200 fs, 200 µJ) set at an effective repetition rate of 1 kHz via an internal pulse picker. A portion of the fundamental (20%) is routed through a double-pass optical delay stage and subsequently used to generate broadband probe pulses (480–900 nm) by focusing on a sapphire crystal. The remainder of the fundamental (80%) is used to pump an optical parametric amplifier (Orpheus-F, Light Conversion) to generate the excitation pulses, which were depolarised and modulated to an average power of 100 µW (100 nJ $pulse^{-1}$). The excitation wavelength was either 340 or 610 nm, as detailed in the results. In order to prevent degradation effects, the film samples were loaded, while in the glovebox, into a home-built airtight holder which was then transferred to the experimental setup. The sample holder was furthermore translated during the measurement (4 $mm^2$ area at 3500 µm $s^{-1}$) to minimize any one part of the film being over exposed to the laser beam. The TA data were analyzed using Surface Xplorer 4.3.0 software.

## Supporting Information

Supporting Information is available from the Wiley Online Library or from the author.

## Acknowledgements

The authors thank C. Bauer, M. Beuchel, F. Keller, S. Koynova, and V. Maus for the technical support and C. Volkert for assistance with the EPR measurement. F.L. thanks the Ingeborg-Gross-Stiftung and the Helmholtz International Research School for Nanoelectronic Networks NanoNet (VH-KO-606).

## Conflict of Interest

The authors declare no conflict of interest.

## Data Availability Statement

The data that supports the findings of this study are available from the corresponding author upon reasonable request.

## Keywords

dihydroazulene, organic memory, organic transistors, photoswitches, stimuli-responsive devices

Received: June 7, 2024
Revised: August 13, 2024
Published online:

[1] C. Wang, Y. Liu, Y. Guo, *Flex. Wear. Electron. Smart Clothing* **2024**, *1*, 41.
[2] H. Sirringhaus, *Adv. Mater.* **2014**, *26*, 1319.
[3] a) M. Nguyen, U. Kraft, W. L. Tan, I. Dobryden, K. Broch, W. Zhang, H.-I. Un, D. Simatos, D. Venkateshavaran, I. McCulloch, P. M. Claesson, C. R. McNeill, H. Sirringhaus, *Adv. Mater.* **2023**, *35*, 2205377; b) H. F. Iqbal, Q. Ai, K. J. Thorley, H. Chen, I. McCulloch, C. Risko, J. E. Anthony, O. D. Jurchescu, *Nat. Commun.* **2021**, *12*, 2352.
[4] S. H. Yu, S. Z. Hassan, C. So, M. Kang, D. S. Chung, *Adv. Mater.* **2023**, *35*, 2203401.
[5] X. Huang, T. Li, *J. Mater. Chem. C* **2020**, *8*, 821.
[6] M. Carroli, A. G. Dixon, M. Herder, E. Pavlica, S. Hecht, G. Bratina, E. Orgiu, P. Samorì, *Adv. Mater.* **2021**, *33*, 2007965.
[7] Q. Huaulmé, V. M. Mwalukuku, D. Joly, J. Liotier, Y. Kervella, P. Maldivi, S. Narbey, F. Oswald, A. J. Riquelme, J. A. Anta, R. Demadrille, *Nat. Energy* **2020**, *5*, 468.
[8] M. Kang, S. Z. Hassan, S.-M. Ko, C. Choi, J. Kim, S. K. R. Parumala, Y.-H. Kim, Y. H. Jang, J. Yoon, D.-W. Jee, D. S. Chung, *Adv. Mater.* **2022**, *34*, 2200526.
[9] Y. Jeon, S. Kim, J. Seo, H. Yoo, *Small Methods* **2024**, *8*, 2300391.
[10] A. Goulet-Hanssens, F. Eisenreich, S. Hecht, *Adv. Mater.* **2020**, *32*, 1905966.
[11] E. Orgiu, P. Samorì, *Adv. Mater.* **2014**, *26*, 1827.
[12] a) L.-N. Fu, B. Leng, Y.-S. Li, X.-K. Gao, *Chin. Chem. Lett.* **2016**, *27*, 1319; b) Y. Wakayama, R. Hayakawa, K. Higashiguchi, K. Matsuda, *J. Mater. Chem. C* **2020**, *8*, 10956; c) C. Xu, J. Zhang, W. Xu, H. Tian, *Mater. Chem. Front.* **2021**, *5*, 1060; d) Y. Wakayama, R. Hayakawa, H.-S. Seo, *Sci. Technol. Adv. Mater.* **2014**, *15*, 024202.
[13] X. Zhang, L. Hou, P. Samorì, *Nat. Commun.* **2016**, *7*, 11118.
[14] Y. Zhao, S. Ippolito, P. Samorì, *Adv. Opt. Mater.* **2019**, *7*, 1900286.
[15] J. Tian, Z. Liu, W. Jiang, D. Shi, L. Chen, X. Zhang, G. Zhang, C.-a. Di, D. Zhang, *Angew. Chem., Int. Ed.* **2020**, *59*, 13844.
[16] Y. Ishiguro, M. Frigoli, R. Hayakawa, T. Chikyow, Y. Wakayama, *Org. Electron.* **2014**, *15*, 1891.
[17] Y. Liu, Y. Yang, D. Shi, M. Xiao, L. Jiang, J. Tian, G. Zhang, Z. Liu, X. Zhang, D. Zhang, *Adv. Mater.* **2019**, *31*, 1902576.
[18] a) E. Orgiu, N. Crivillers, M. Herder, L. Grubert, M. Pätzel, J. Frisch, E. Pavlica, D. T. Duong, G. Bratina, A. Salleo, N. Koch, S. Hecht, P. Samorì, *Nat. Chem.* **2012**, *4*, 675; b) M. E. Gemayel, K. Börjesson, M. Herder, D. T. Duong, J. A. Hutchison, C. Ruzié, G. Schweicher, A. Salleo, Y. Geerts, S. Hecht, E. Orgiu, P. Samorì, *Nat. Commun.* **2015**, *6*, 6330.
[19] a) Q. Shen, L. Wang, S. Liu, Y. Cao, L. Gan, X. Guo, M. L. Steigerwald, Z. Shuai, Z. Liu, C. Nuckolls, *Adv. Mater.* **2010**, *22*, 3282; b) J.-J. Lv, X. Gao, L.-X. Zhang, Y. Feng, J.-L. Xu, J. Xiao, B. Dong, S.-D. Wang, *Appl. Phys. Lett.* **2019**, *115*, 113302.
[20] a) T. Mosciatti, M. G. del Rosso, M. Herder, J. Frisch, N. Koch, S. Hecht, E. Orgiu, P. Samorì, *Adv. Mater.* **2016**, *28*, 6606; b) S. H. Yu, S. Z. Hassan, G.-H. Nam, S. An, B. Kang, D. S. Chung, *Chem. Mater.* **2021**, *33*, 5991.
[21] a) H. Zhang, X. Guo, J. Hui, S. Hu, W. Xu, D. Zhu, *Nano Lett.* **2011**, *11*, 4939; b) H. Chen, N. Cheng, W. Ma, M. Li, S. Hu, L. Gu, S. Meng, X. Guo, *ACS Nano* **2016**, *10*, 436.
[22] a) J. Tian, Z. Liu, C. Wu, W. Jiang, L. Chen, D. Shi, X. Zhang, G. Zhang, D. Zhang, *Adv. Mater.* **2021**, *33*, 2005613; b) M. Li, J. Zheng, X. Wang, R. Yu, Y. Wang, Y. Qiu, X. Cheng, G. Wang, G. Chen, K. Xie, J. Tang, *Nat. Commun.* **2022**, *13*, 4912.
[23] H. Zhang, J. Hui, H. Chen, J. Chen, W. Xu, Z. Shuai, D. Zhu, X. Guo, *Adv. Electron. Mater.* **2015**, *1*, 1500159.
[24] a) L. A. Frolova, A. A. Rezvanova, V. Z. Shirinian, A. G. Lvov, A. V. Kulikov, M. M. Krayushkin, P. A. Troshin, *Adv. Electron. Mater.* **2016**, *2*, 1500219; b) F. A. Obrezkov, D. D. Dashitsyrenova, A. G. Lvov, D. Y. Volyniuk, V. Z. Shirinian, P. Stadler, J. V. Grazulevicius, N. S. Sariciftci, S. M. Aldoshin, M. M. Krayushkin, P. A. Troshin, *ACS Appl. Mater. Interfaces* **2020**, *12*, 32987.

[25] a) Y. Ishiguro, R. Hayakawa, T. Yasuda, T. Chikyow, Y. Wakayama, *ACS Appl. Mater. Interfaces* **2013**, *5*, 9726; b) Y. Ishiguro, R. Hayakawa, T. Chikyow, Y. Wakayama, *ACS Appl. Mater. Interfaces* **2014**, *6*, 10415; c) Y. Ishiguro, R. Hayakawa, T. Chikyow, Y. Wakayama, *J. Mater. Chem. C* **2013**, *1*, 3012; d) J. Ma, J. Tian, Z. Liu, D. Shi, X. Zhang, G. Zhang, D. Zhang, *CCS Chem.* **2020**, *2*, 632.

[26] S. L. Broman, M. B. Nielsen, *Phys. Chem. Chem. Phys.* **2014**, *16*, 21172.

[27] A. Plaquet, B. Champagne, F. Castet, L. Ducasse, E. Bogdan, V. Rodriguez, J.-L. Pozzo, *New J. Chem.* **2009**, *33*, 1349.

[28] a) S. Lara-Avila, A. V. Danilov, S. E. Kubatkin, S. L. Broman, C. R. Parker, M. B. Nielsen, *J. Phys. Chem. C* **2011**, *115*, 18372; b) C. Huang, M. Jevric, A. Borges, S. T. Olsen, J. M. Hamill, J.-T. Zheng, Y. Yang, A. Rudnev, M. Baghernejad, P. Broekmann, A. U. Petersen, T. Wandlowski, K. V. Mikkelsen, G. C. Solomon, M. Brøndsted Nielsen, W. Hong, *Nat. Commun.* **2017**, *8*, 15436; c) S. L. Broman, S. Lara-Avila, C. L. Thisted, A. D. Bond, S. Kubatkin, A. Danilov, M. B. Nielsen, *Adv. Funct. Mater.* **2012**, *22*, 4249; d) S. T. Olsen, T. Hansen, M. B. Nielsen, M. A. Ratner, K. V. Mikkelsen, *J. Phys. Chem. C* **2017**, *121*, 3163; e) C.-J. Xia, A.-Y. Yang, B.-Q. Zhang, Y. H. Su, Z.-Y. Tu, J. Wang, *Mol. Phys.* **2017**, *115*, 1606.

[29] a) K. H. Au-Yeung, T. Kühne, O. Aiboudi, S. Sarkar, O. Guskova, D. A. Ryndyk, T. Heine, F. Lissel, F. Moresco, *Nanoscale Adv* **2022**, *4*, 4351; b) T. Kühne, K. H. Au-Yeung, F. Eisenhut, O. Aiboudi, D. A. Ryndyk, G. Cuniberti, F. Lissel, F. Moresco, *Nanoscale* **2020**, *12*, 24471.

[30] T. Li, M. Jevric, J. R. Hauptmann, R. Hviid, Z. Wei, R. Wang, N. E. A. Reeler, E. Thyrhaug, S. Petersen, J. A. S. Meyer, N. Bovet, T. Vosch, J. Nygård, X. Qiu, W. Hu, Y. Liu, G. C. Solomon, H. G. Kjaergaard, T. Bjørnholm, M. B. Nielsen, B. W. Laursen, K. Nørgaard, *Adv. Mater.* **2013**, *25*, 4164.

[31] a) J. Daub, T. Knöchel, A. Mannschreck, *Angew. Chem. Int. Edit. Eng.* **1984**, *23*, 960; b) S. Gierisch, J. Daub, *Chem. Ber.* **1989**, *122*, 69; c) J. Daub, S. Gierisch, U. Klement, T. Knöchel, G. Maas, U. Seitz, *Chem. Ber.* **1986**, *119*, 2631.

[32] a) H. Görner, C. Fischer, S. Gierisch, J. Daub, *J. Phys. Chem.* **1993**, *97*, 4110; b) H. Görner, C. Fischer, J. Daub, *J. Photochem. Photobiol. A Chem.* **1995**, *85*, 217.

[33] S. L. Broman, S. L. Brand, C. R. Parker, M. Å. Petersen, C. G. Tortzen, A. Kadziola, K. Kilså, M. B. Nielsen, *ARKIVOC* **2011**, *137*, 51.

[34] Z. Fei, P. Boufflet, S. Wood, J. Wade, J. Moriarty, E. Gann, E. L. Ratcliff, C. R. McNeill, H. Sirringhaus, J.-S. Kim, M. Heeney, *J. Am. Chem. Soc.* **2015**, *137*, 6866.

[35] a) N. Crivillers, E. Orgiu, F. Reinders, M. Mayor, P. Samorì, *Adv. Mater.* **2011**, *23*, 1447; b) Q. Shen, Y. Cao, S. Liu, M. L. Steigerwald, X. Guo, *J. Phys. Chem. C* **2009**, *113*, 10807.

[36] J.-M. Zhuo, L.-H. Zhao, R.-Q. Png, L.-Y. Wong, P.-J. Chia, J.-C. Tang, S. Sivaramakrishnan, M. Zhou, E. C. W. Ou, S.-J. Chua, W.-S. Sim, L.-L. Chua, P. K. H. Ho, *Adv. Mater.* **2009**, *21*, 4747.

[37] a) X. Ruan, S. Cheng, W. Deng, Y. Tan, Z. Lu, J. Shi, X. Zhang, J. Jie, *Adv. Electron. Mater.* **2022**, *8*, 2200355; b) D. Simatos, I. E. Jacobs, I. Dobryden, M. Nguyen, A. Savva, D. Venkateshvaran, M. Nikolka, J. Charmet, L. J. Spalek, M. Gicevičius, Y. Zhang, G. Schweicher, D. J. Howe, S. Ursel, J. Armitage, I. B. Dimov, U. Kraft, W. Zhang, M. Alsufyani, I. McCulloch, R. M. Owens, P. M. Claesson, T. P. J. Knowles, H. Sirringhaus, *Small Methods* **2023**, *7*, 2300476.

[38] S. L. Broman, M. Jevric, M. B. Nielsen, *Chemistry* **2013**, *19*, 9542.

[39] M. Hanazawa, R. Sumiya, Y. Horikawa, M. Irie, *J. Chem. Soc., Chem. Commun.* **1992**, 206.

[40] H. Jean-Ruel, R. R. Cooney, M. Gao, C. Lu, M. A. Kochman, C. A. Morrison, R. J. Miller, *J Phys Chem A* **2011**, *115*, 13158.

[41] A. Gonzalez, E. S. Kengmana, M. V. Fonseca, G. G. Han, *Mater. Today Adv.* **2020**, *6*, 100058.

[42] L. Hou, T. Leydecker, X. Zhang, W. Rekab, M. Herder, C. Cendra, S. Hecht, I. McCulloch, A. Salleo, E. Orgiu, P. Samorì, *J. Am. Chem. Soc.* **2020**, *142*, 11050.

[43] Y. Chen, H. Wang, H. Chen, W. Zhang, S. Xu, M. Pätzel, C. Ma, C. Wang, I. McCulloch, S. Hecht, P. Samorì, *Adv. Funct. Mater.* **2023**, *33*, 2305494.

[44] L. Ma, W. H. Lee, Y. D. Park, J. S. Kim, H. S. Lee, K. Cho, *Appl. Phys. Lett.* **2008**, *92*, 063310.

[45] A. F. Paterson, N. D. Treat, W. Zhang, Z. Fei, G. Wyatt-Moon, H. Faber, G. Vourlias, P. A. Patsalas, O. Solomeshch, N. Tessler, M. Heeney, T. D. Anthopoulos, *Adv. Mater.* **2016**, *28*, 7791.

[46] S. P. Tiwari, W. J. Potscavage, T. Sajoto, S. Barlow, S. R. Marder, B. Kippelen, *Org. Electron.* **2010**, *11*, 860.

[47] J. E. Lyon, A. J. Cascio, M. M. Beerbom, R. Schlaf, Y. Zhu, S. A. Jenekhe, *Appl. Phys. Lett.* **2006**, *88*, 222109.

[48] I. McCulloch, M. Heeney, C. Bailey, K. Genevicius, I. MacDonald, M. Shkunov, D. Sparrowe, S. Tierney, R. Wagner, W. Zhang, M. L. Chabinyc, R. J. Kline, M. D. McGehee, M. F. Toney, *Nat. Mater.* **2006**, *5*, 328.

[49] A. D. Scaccabarozzi, A. Basu, F. Aniés, J. Liu, O. Zapata-Arteaga, R. Warren, Y. Firdaus, M. I. Nugraha, Y. Lin, M. Campoy-Quiles, N. Koch, C. Müller, L. Tsetseris, M. Heeney, T. D. Anthopoulos, *Chem. Rev.* **2022**, *122*, 4420.

[50] M. Balcı Leinen, P. Klein, F. L. Sebastian, N. F. Zorn, S. Adamczyk, S. Allard, U. Scherf, J. Zaumseil, *Adv. Electron. Mater.* **2020**, *6*, 2000717.

[51] M.-N. Chen, C.-Y. Ke, A. Nyayachavadi, H. Zhao, M. U. Ocheje, M. Mooney, Y.-T. Li, X. Gu, G.-S. Liou, S. Rondeau-Gagné, Y.-C. Chiu, *ACS Appl. Mater. Interfaces* **2023**, *15*, 53755.

[52] a) L.-N. Fu, B. Leng, Y.-S. Li, X.-K. Gao, *Chin. Chem. Lett.* **2018**, *29*, 175; b) Y. Bardavid, I. Goykhman, D. Nozaki, G. Cuniberti, S. Yitzchaik, *J. Phys. Chem. C* **2011**, *115*, 3123.

[53] L. Gobbi, P. Seiler, F. Diederich, V. Gramlich, C. Boudon, J.-P. Gisselbrecht, M. Gross, *Helv. Chim. Acta* **2001**, *84*, 743.

[54] a) J. Daub, C. Fischer, S. Gierisch, J. Set, *Section A. Mol. Cryst. Liquid Cryst.* **1992**, *217*, 177; b) J. Daub, J. Salbeck, T. Knöchel, C. Fischer, H. Kunkely, K. M. Rapp, *Ang. Chemie Int. Edit. in Engl.* **1989**, *28*, 1494.

[55] C. Fischer, J. Daub, *Chem. Ber.* **1993**, *126*, 1631.

[56] M. Nikolka, I. Nasrallah, B. Rose, M. K. Ravva, K. Broch, A. Sadhanala, D. Harkin, J. Charmet, M. Hurhangee, A. Brown, S. Illig, P. Too, J. Jongman, I. McCulloch, J.-L. Bredas, H. Sirringhaus, *Nat. Mater.* **2017**, *16*, 356.

[57] M. Nikolka, G. Schweicher, J. Armitage, I. Nasrallah, C. Jellett, Z. Guo, M. Hurhangee, A. Sadhanala, I. McCulloch, C. B. Nielsen, H. Sirringhaus, *Adv. Mater.* **2018**, *30*, 1801874.

[58] J. Armitage, L. J. Spalek, M. Nguyen, M. Nikolka, I. E. Jacobs, L. Marañón, I. Nasrallah, G. Schweicher, I. Dimov, D. Simatos, I. McCulloch, C. B. Nielsen, G. Conduit, H. Sirringhaus, *ArXiv* **2019**, arXiv:1910.13325.

[59] D. Simatos, L. J. Spalek, U. Kraft, M. Nikolka, X. Jiao, C. R. McNeill, D. Venkateshvaran, H. Sirringhaus, *APL Mater.* **2021**, *9*, 041113.

[60] Z. A. Lamport, H. F. Haneef, S. Anand, M. Waldrip, O. D. Jurchescu, *J. Appl. Phys.* **2018**, *124*, 071101.